UNIVERSITY OF ALBERTA

The Ionospheric Feedback Instability Revisited

- W. Shen, R. Rankin, and D. Sydorenko

University of Alberta, Edmonton, Canada.

UNIVERSITY OF ALBERTA

CONTENTS

UNIVERSITY OF ALBERTA

PART ONE

Introduction

Introduction-very brief history of IFI

University of Alberta

- IFI – much postulated as a mechanism for forming narrow filaments auroral precipitation or spontaneous formation of auroral arcs.
- IFI was first introduced by Atkinson [JGR, 1970] and Sato [JGR, 1978], subsequent studies were published by Miura and Sato, JGR, 1980; Lysak, JGR, 1991; Streltsov, JGR, 2008; etc.
- With very few exceptions, published theory of the IFI treat the ionosphere as a height-integrated conductivity (HIC) sheet and omits wave propagation within it.
- Recent numerical simulations of the IFI in a resolved realistic ionosphere show no evidence of the instability [Sydorenko and Rankin, GRL, 2017].
- Watanabe [GRL, 2018 & PoP, 2023] used a simplified model of flow shear in the E-region and refuted the claim that IFI is stabilized.

Introduction-our goals

UNIVERSITY OF ALBERTA

- We investigate IFI, discuss the stabilizing influence of the ionosphere on the IFI and confirm the findings of SR. An analysis is presented based on eigenmode analysis with HIC and resolved layer boundary conditions.
- Results are presented for field line resonances and waves excited in the IAR.
- Dispersion properties of IFI wave modes are presented for fully-resolved, partially resolved, and height-integrated layers of the ionosphere.

PART TWO

Model

Model-geometry

UNIVERSITY OF ALBERTA

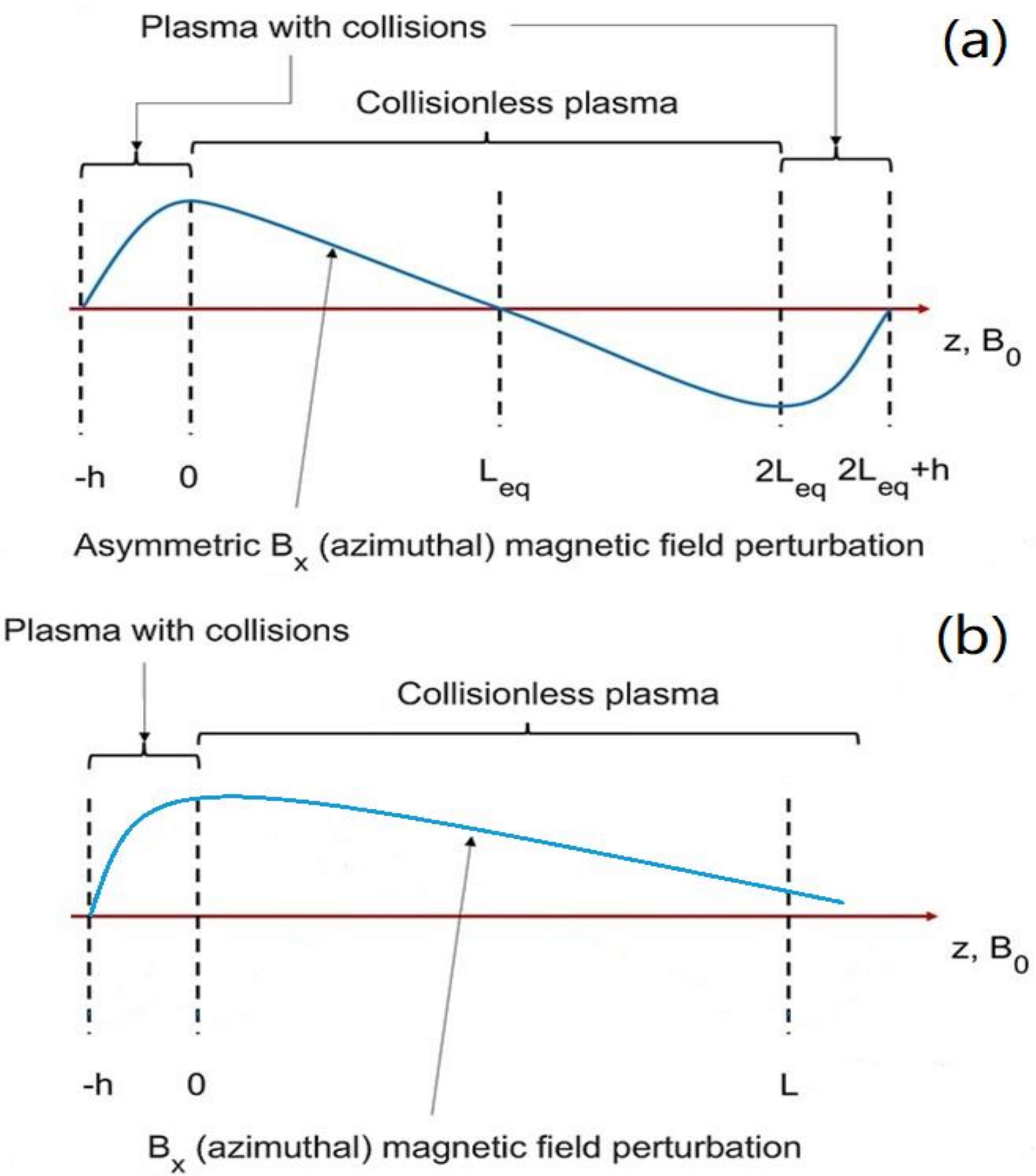

FIG 2. Geometry and regions of interest for long-period FLRs (a), and higher-frequency waves in the IAR (b).

Model-coupled ODEs and boundary conditions

$$\frac{d\tilde{E}_y}{dz} = -i\omega\tilde{B}_x\left(1+\frac{c^2{k_y}^2}{{\omega_{pe}}^2}\right)+\frac{c^2{k_y}^2}{{\omega_{pe}}^2}\nu_{en}\tilde{B}_x$$

$$\left(\omega - k_y\mu_p E_0\right)\frac{d\tilde{B}_x}{dz} = -\omega\left(i\omega\frac{F}{V_A^2} - \mu_0 e\mu_p n_0\right)\tilde{E}_y$$

BCs: For FLRs, $\tilde{B}_x = 0$ at the equator. For IAR, the Alfven wave boundary conditions at the upper boundary are defined by:

$$\frac{E_y}{B_x} = V_A\sqrt{1+k_y^2\lambda_e^2} = V_A\sqrt{1+k_y^2c^2/\omega_{pe}^2}$$

The BC used at the bottom of the E-layer, corresponds to $\tilde{B}_x = 0$ at $z = -h$.

Model-coupled ODEs and boundary conditions

$$\frac{1}{\mu_0}\frac{\partial B_x}{\partial t}\bigg|_{z=s-h} = \frac{\partial}{\partial t}\int_{-h}^{s-h} dzen_0\mu_P E_y + \frac{\partial^2}{\partial t^2}\int_{-h}^{s-h} dzen_0\frac{F}{\Omega_i B_0}E_y - \frac{E_0}{\mu_0}\frac{\partial}{\partial y}\int_{-h}^{s-h} dz\mu_P\frac{\partial B_x}{\partial z}$$

$$(\omega - \langle\mu_P\rangle E_0 k_y)\,\tilde{B}_x\Big|_{z=s-h} = \mu_0(\omega\Sigma_P - i\omega^2\Sigma_A)\,\tilde{E}_y\Big|_{z=s-h}$$

$$\langle\mu_P\rangle = \frac{1}{s}\int_{-h}^{s-h} dz\mu_P$$

$$\Sigma_P = \int_{-h}^{s-h} dzen_0\mu_P$$

$$\Sigma_A = \int_{-h}^{s-h} dzen_0\frac{F}{\Omega_i B_0}$$

The calculations can proceed only if E_y is constant, which is normally true and if $B_x \propto z$, which is not true in general.

UNIVERSITY OF ALBERTA

PART THREE

Results

Results-system parameters

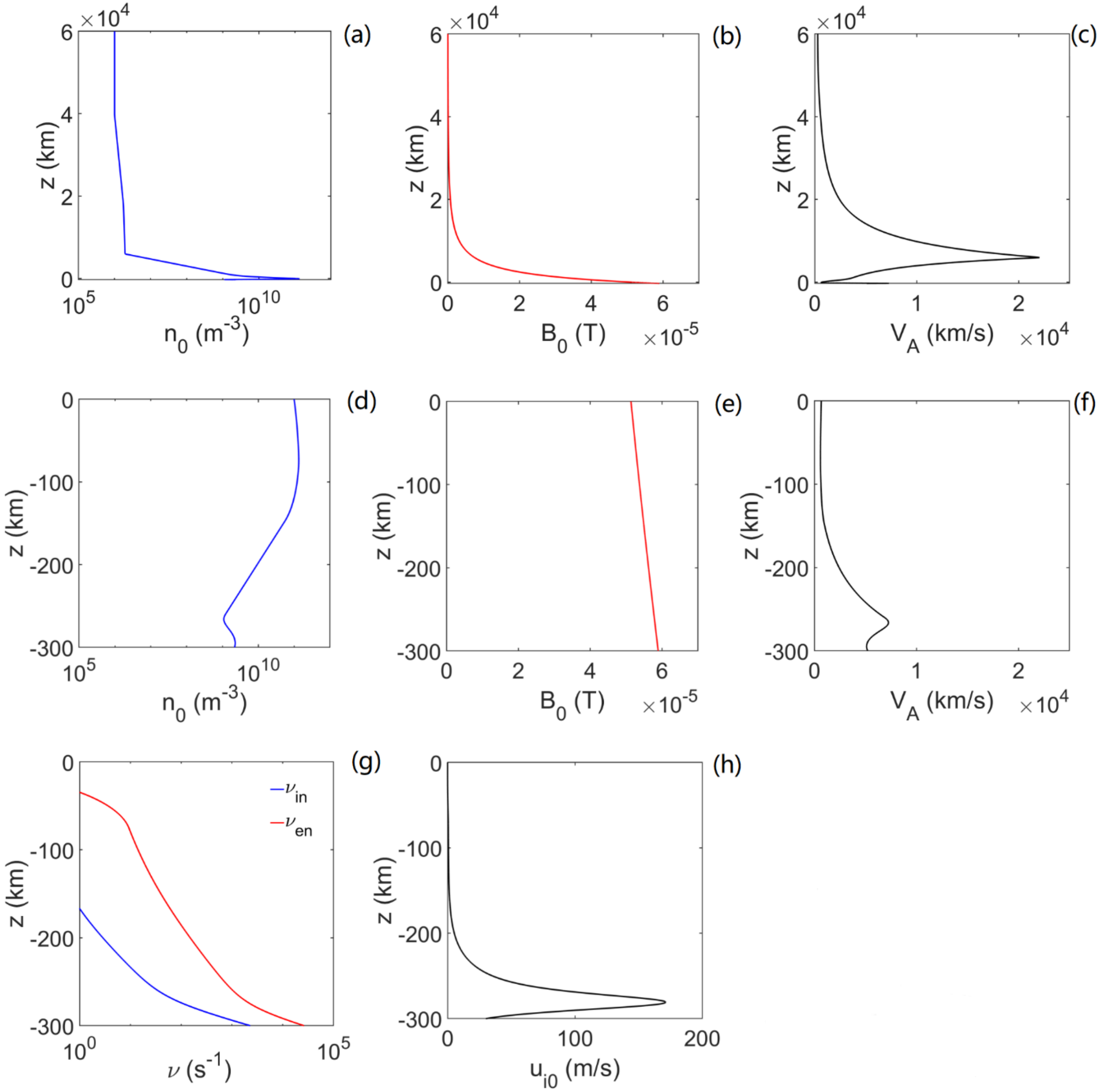

FIG 3. Panels (a)(d), (b)(e), and (c)(f) display ambient plasma density, magnetic field, and Alfvén speed, respectively. The top row shows parameters in the ionosphere-magnetosphere coupling system, while the middle row shows an expanded view of the ionosphere region. Panel (g)(h) show the variation of collision frequencies and ion drift velocities. $L_s = 7.59, E_0 = 20$ mVm^{-1} .

Results-dispersion curves for FLRs

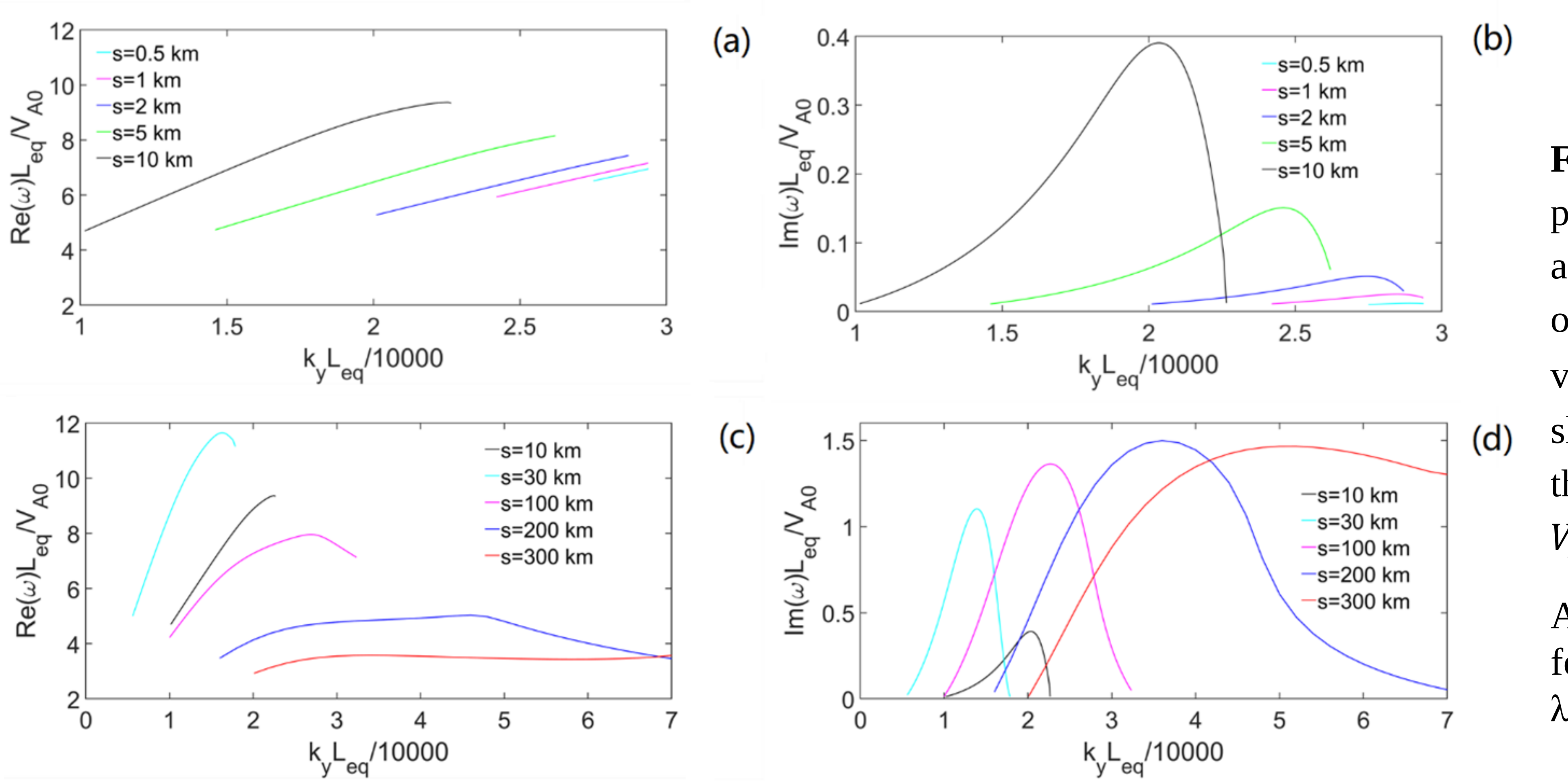

FIG 4. Curves in each panel show the real (a, c) and imaginary (b, d) parts of the wave frequency versus k_y for thin HIC slab thicknesses (a, b) and thicker thicknesses (c, d). $V_{A0} = 130.82$ km/s.

At the growth rate peak for $s = 300$ km, we have λ~7.5 km and T ~1000 s.

Results-eigenfunctions for FLRs

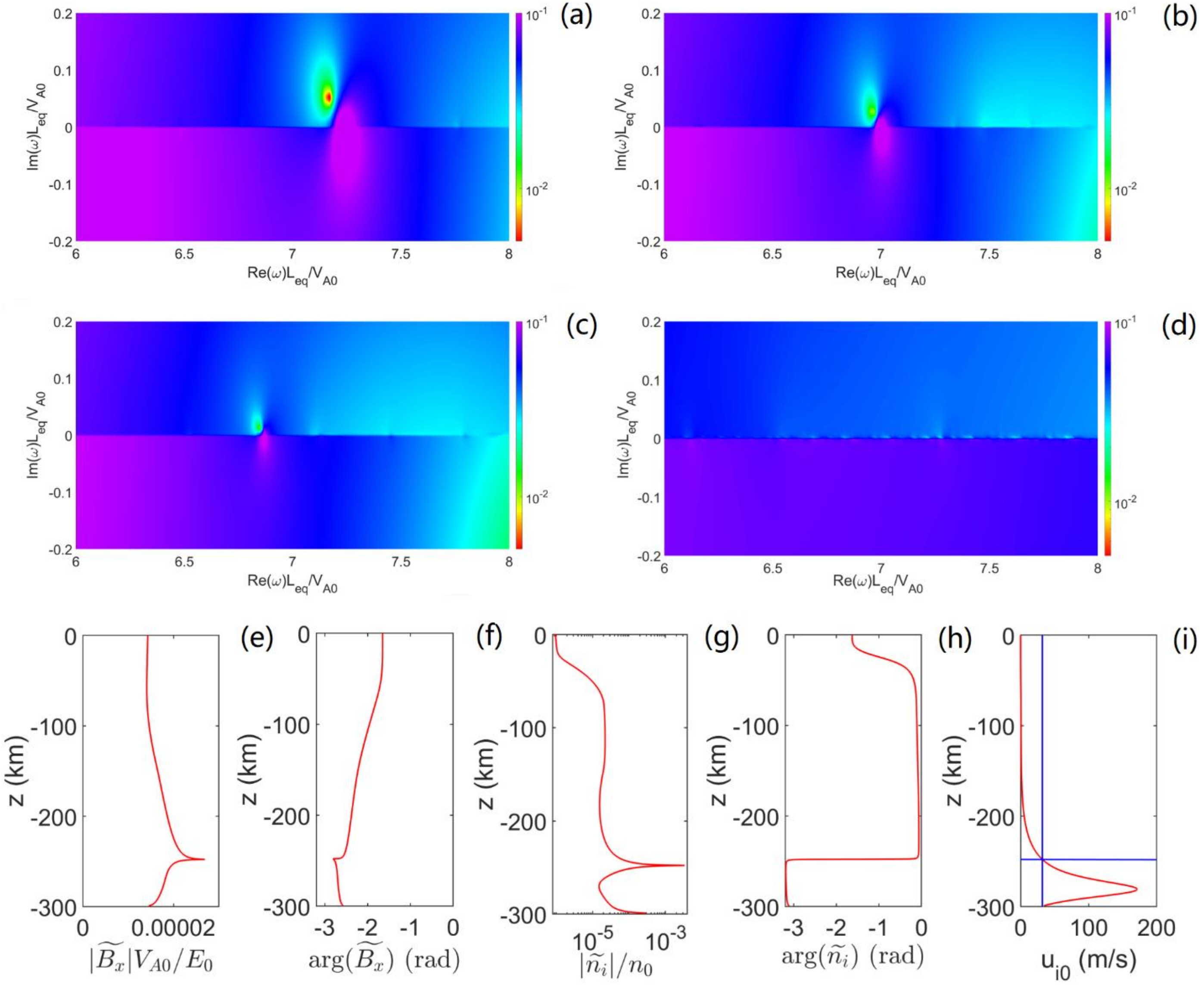

FIG 5. The top and middle rows demonstrate the absolute value of the perturbed magnetic field $\tilde{B}_x$ in the equatorial plane. Absolute value (e) and argument (f) of $\tilde{B}_x$; absolute value (g) and argument (h) of the perturbed density $\tilde{n}_i$; ambient horizontal ion flow velocity u_{i0} (i) vs z inside the ionosphere for $s = 1$ km case are shown in the bottom row.

Results-FLRs, artificial collision profiles

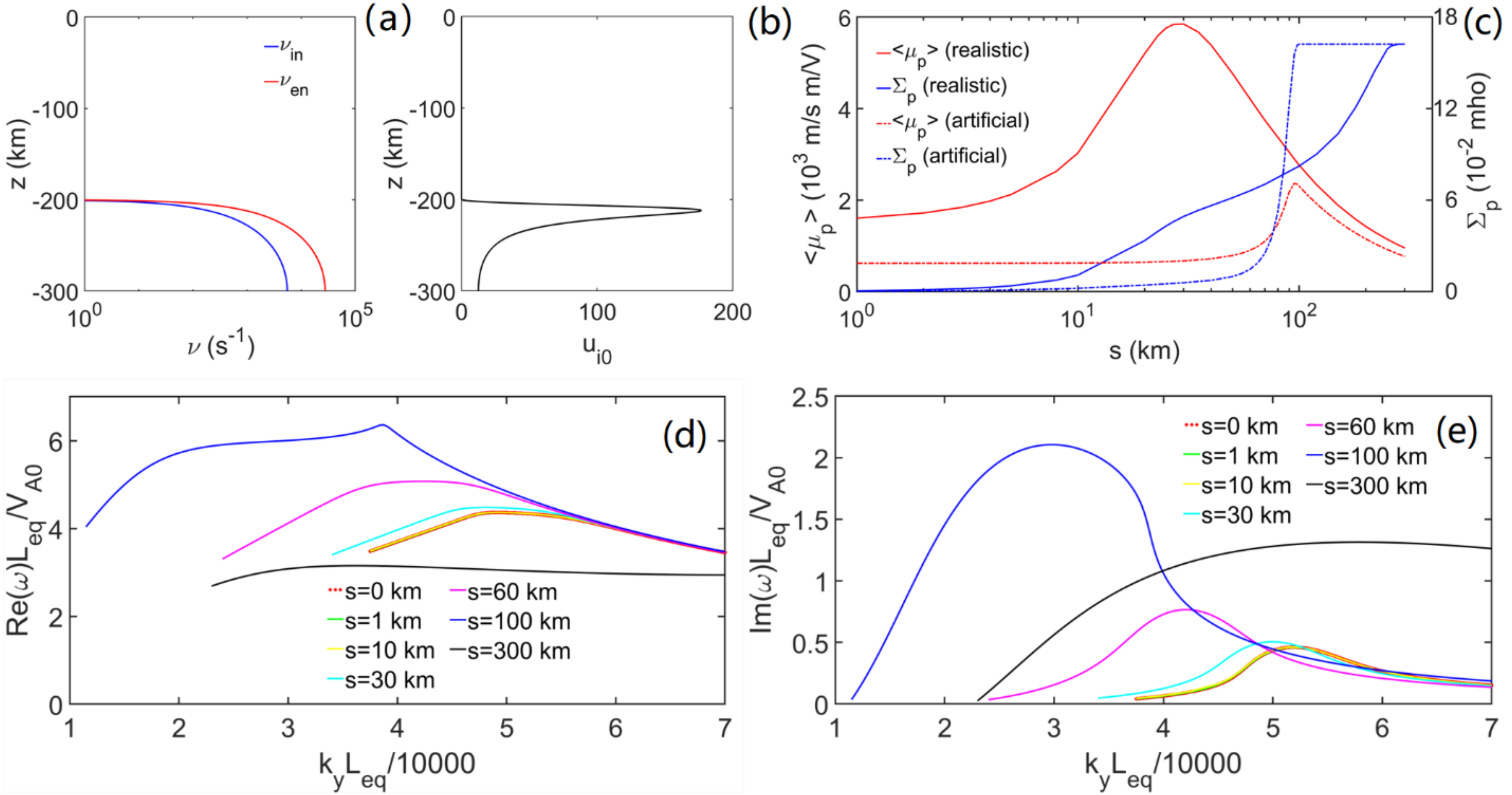

FIG 6. Simulation parameters for the artificial collision profiles inside the ionosphere are displayed in the top row. Panels (d) and (e) show real and imaginary parts of the wave frequency versus k_y with the artificial collision frequency profiles, respectively.

Results-dispersion curves for IAR

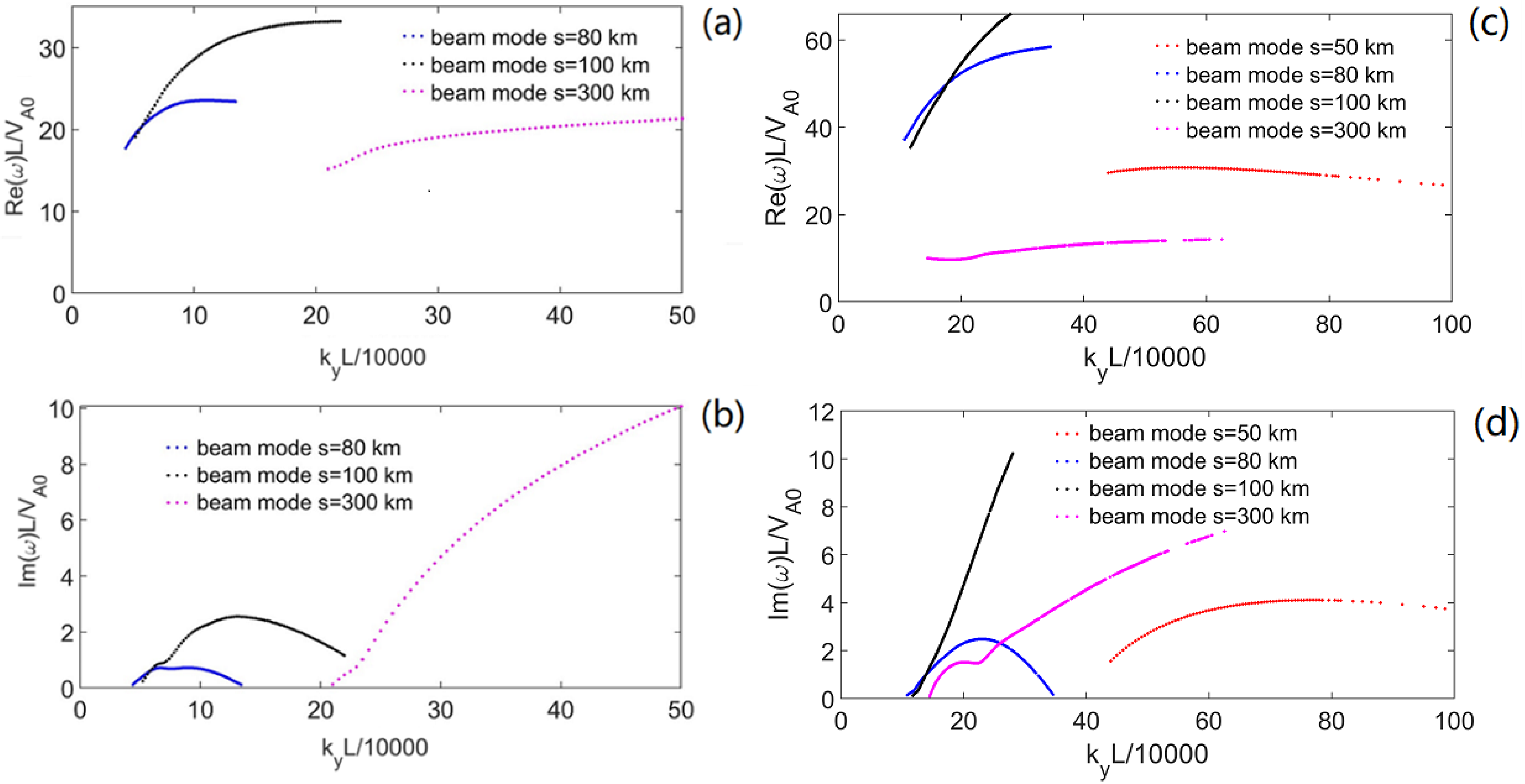

FIG 7. Panels (a)(b) display beam mode branches with $E_0 = 80$ mV/s but various HIC boundary conditions (i.e., different values of s), for the system with summer nighttime collision and density profiles (0.192 mho). Panel (c)(d) show those modes calculated from the winter nighttime ionosphere (0.064 mho). L = 5000 km.

At the growth rate peak for $s = 80$ km, we have λ~1 km and T ~2 s.

Results-dispersion curves for IAR (non-IFI instabilities)

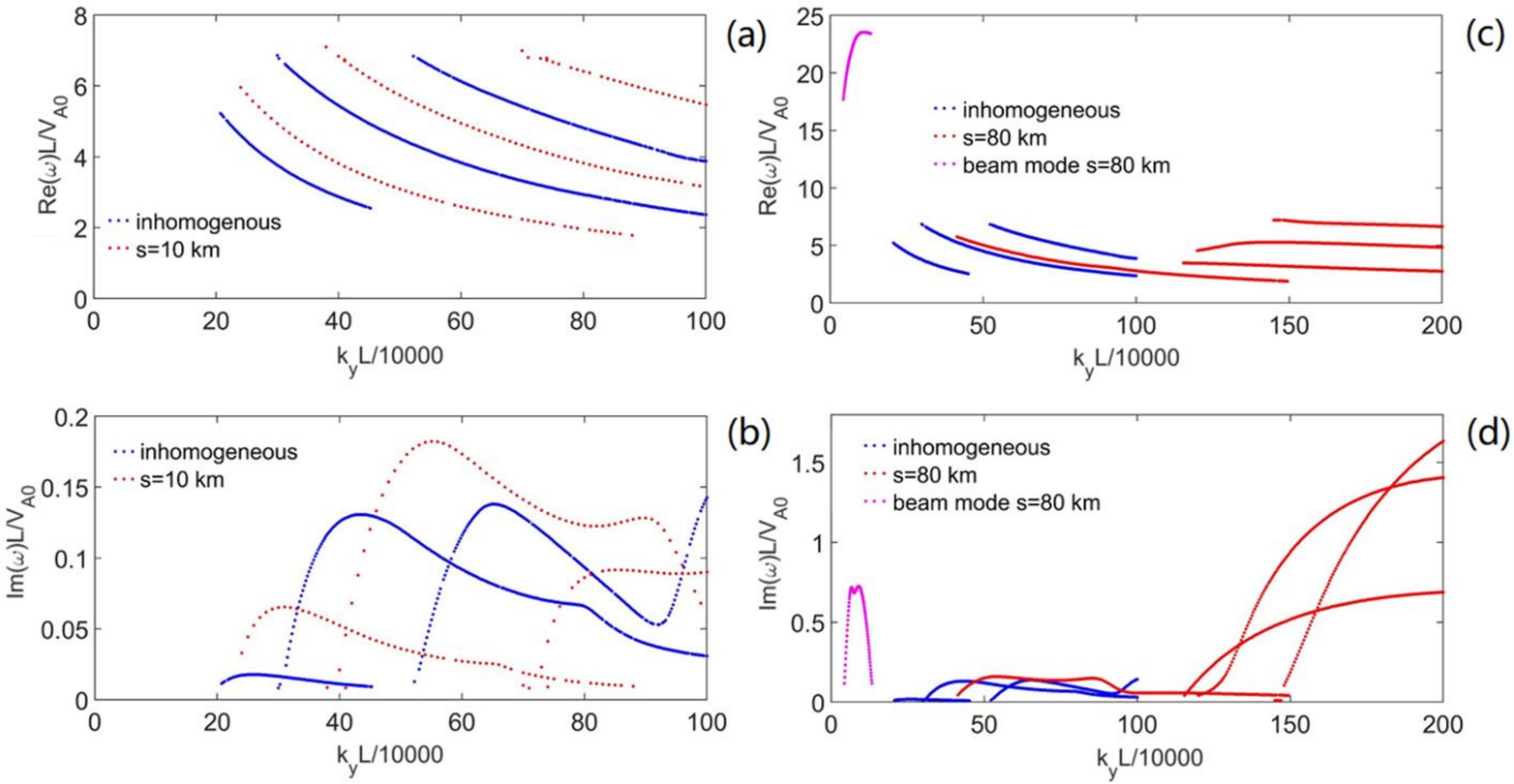

FIG 8. Panels (a)(b) show the non-IFI instable modes for a height resolved ionosphere as well as the shift of the branches for $s = 10$ km. While panels (c)(d) demonstrate the dispersion relationships for $s = 80$ km, the IFI branches are shown in purple.

UNIVERSITY OF ALBERTA

PART FOUR

Conclusions

Conclusions

- The reduction in growth rates of the ionospheric feedback instability occurs for both long-period FLRs and IAR. The reason for this is the strong nonlinearity of magnetic field and plasma density perturbation profiles along with the horizontal collision-induced ion flow shear.
- The IFI results are highly collision profile dependent, therefore, collisional simulation parameters should be cautiously chosen in relevant investigations. The results of Watanabe are unreliable as he used an unjustified and flawed treatment of collision profiles.
- BOTTOM LINE: IFI, whether you believe it exists or not, should include effects of the ionosphere (e.g., height resolved cross field ion flow) beyond the HIC assumption. Adopting a full HIC boundary condition is not valid with a realistic ionosphere we investigated.

Thanks!

Presented by Wei

wshen2@ualberta.ca

Introduction-physical picture of IFI

In an ionosphere with strong convection, ionospheric perturbations emit upward Alfven waves.

Waves reflect from Alfven speed gradient and propagate downward.

Reflected waves arrive at locations of existing perturbations and amplify them.

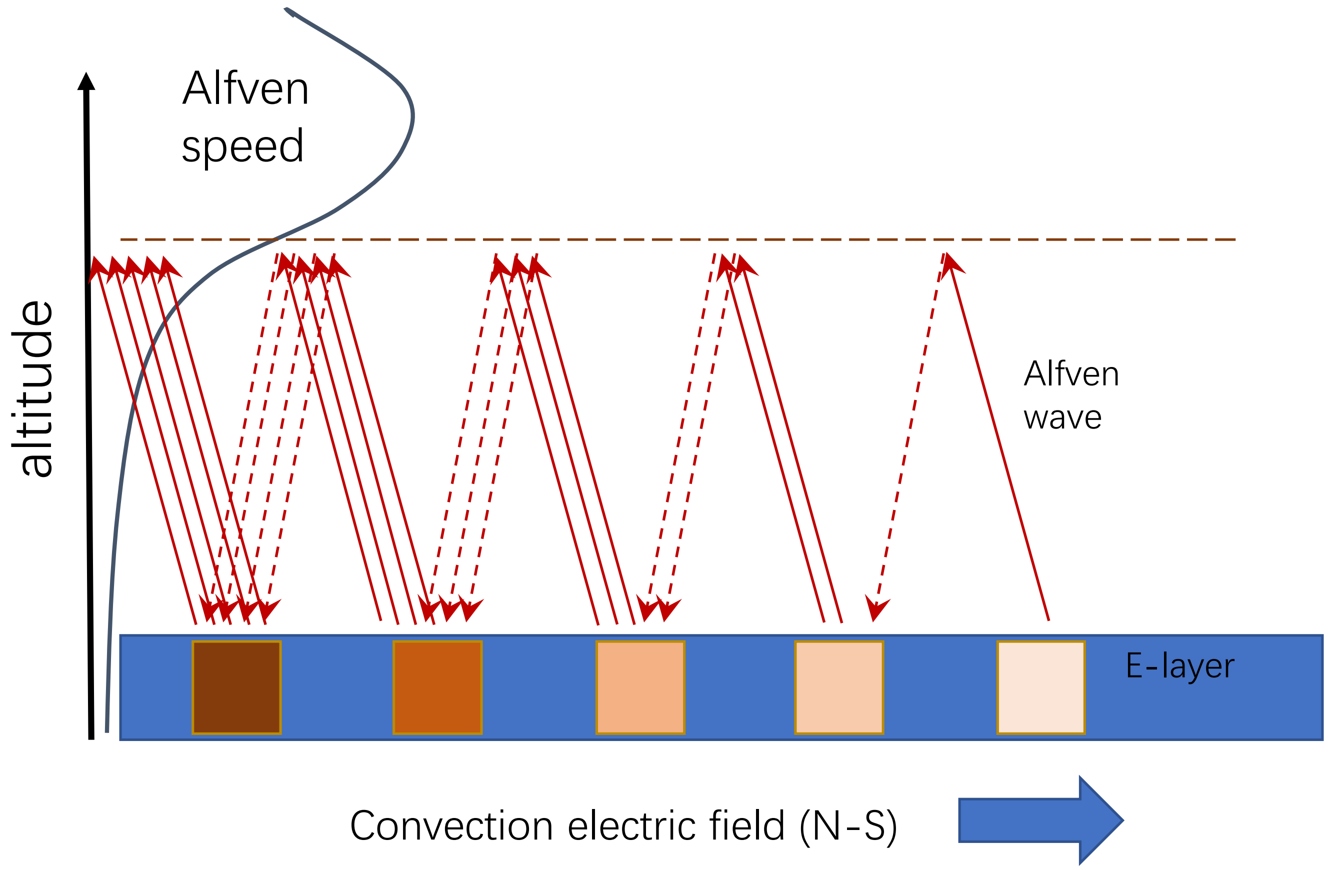

FIG 1. Physical picture of the IFI (in IAR)